analytical chemistry

Article

pubs.acs.org/ac

Simultaneous Analysis of Hydrodynamic and Optical Properties Using Analytical Ultracentrifugation Equipped with Multiwavelength Detection

Johannes Walter,[†] Peter J. Sherwood,[‡] Wei Lin,[†] Doris Segets,[†] Walter F. Stafford,*[,§] and Wolfgang Peukert*[,†]

[†]Friedrich-Alexander-Universität Erlangen-Nürnberg (FAU), Institute of Particle Technology (LFG), Cauerstrasse 4, 91058 Erlangen, Bavaria, Germany

[‡]Interactive Technology Inc., P.O. Box 2768, Oakland, California 94602, United States

[§]Boston Biomedical Research Institute, c/o 12 Francis Avenue, Cambridge, Massachusetts 02138, United States

Supporting Information

ABSTRACT: Analytical ultracentrifugation (AUC) has proven to be a powerful tool for the study of particle size distributions, particle shapes, and interactions with high accuracy and unrevealed resolution. In this work we show how the analysis of sedimentation velocity data from the AUC equipped with a multiwavelength detector (MWL) can be used to gain an even deeper understanding of colloidal and macromolecular mixtures. New data evaluation routines have been integrated in the software SEDANAL to allow for the handling of MWL data. This opens up a variety of new possibilities because spectroscopic information becomes available for individual components in mixtures at the same time using MWL-AUC. For systems of known optical properties information on the hydrodynamic properties of the individual components in a mixture becomes accessible. For the first time, the determination of individual extinction spectra of components in mixtures is demonstrated via MWL evaluation of sedimentation velocity data. In our paper we first provide the informational background for the data analysis and expose the accessible parameters of our methodology. We further demonstrate the data evaluation by means of simulated data. Finally, we give two examples which are highly relevant in the field of nanotechnology using colored silica and gold nanoparticles of different size and extinction properties.

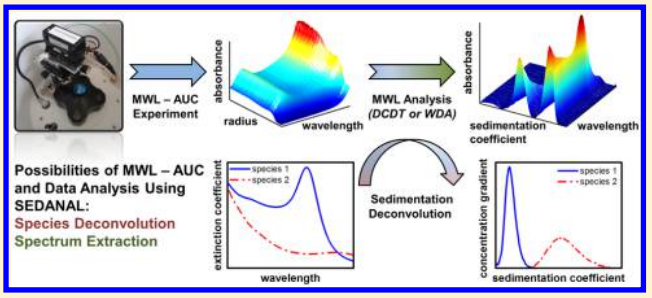

The in-depth characterization of disperse properties is more than ever indispensable for applications in biomedicine and nanotechnology. Product properties are driven by intermolecular interactions, particle size and shape distributions as well as optical properties. A deep understanding of the structure−property relations is required to tune the product properties in a targeted manner. Moreover, biocompatibility and the field of degenerative diseases are also dependent upon the disperse properties of macromolecules and nanoparticles (NPs) in solution. This includes interactions and surface modifications of NPs with proteins but also shape anisotropy. Thus, versatile and accurate techniques are required to address the characterization of a large variety of disperse systems.

It has been demonstrated that analytical ultracentrifugation (AUC) can provide accurate access to these questions by means of sedimentation velocity (SV) experiments.[1,2] In a SV experiment, the temporal and spatial propagation of the sedimentation boundary is recorded and is then linked to the hydrodynamic properties of the individual components. AUC requires only a sample volume of <400 μL and is nondestructive. It has a very high statistical confidence compared to ensemble-based techniques such as dynamic light scattering because even minor fractions of the dispersed system are detected. Additionally, due to the inherent fractionation, a very high dynamic range in combination with an outstanding accuracy is obtained.[2−6]

Recently, the possibilities of AUC have been further expanded by means of multiwavelength (MWL) detection, which adds a further dimension to the data.[5,7,8] This opens up new capabilities of data analysis because structure−property relations can be investigated with respect to the different extinction properties of the analytes. For systems of known optical properties, particle and protein interactions could be studied with higher accuracy because different components can be distinguished by means of their extinction properties. Another interesting application is the determination of optical properties of individual species in mixtures. This is highly relevant for industrial and academic applications because many systems are polydisperse after synthesis and minor fractions can be detected. In polydisperse

Received: December 15, 2014
Accepted: February 13, 2015
Published: February 13, 2015

DOI: 10.1021/ac504649c
Anal. Chem. 2015, 87, 3396−3403

samples, a direct correlation of, e.g., particle size and spectral properties is then not possible any more because the underlying distributions interfere with each other. Highly time-consuming purification methods – provided they are available at all – have to be applied to isolate and investigate the extinction properties of the different components. However, since AUC is based on fractionation of particles in a centrifugal field optical properties now become accessible via MWL detection without any tedious prepurification steps. In a recent study, it was shown that MWL detection allows for the analysis and discrimination of hydrodynamic and optical properties in one experiment with high accuracy.[5] However, due to a lack of data analysis software, only qualitative evaluations could be carried out, and it was not possible to isolate the full extinction spectra of the individual components from a sedimentation velocity experiment.

Unfortunately, until now no data evaluation routines are available to fully handle such novel MWL data. However, the development of new software and algorithms is indispensable to benefit from the new opportunities provided by MWL-AUC. The AUC analysis tools Sedfit,[9] Sedphat,[9] and SEDANAL[10,11] offer possibilities of multisignal analysis based on a commercial absorbance detector, which can record up to three wavelengths in a row. Balbo et al. have demonstrated that the spectral discrimination can synergistically enhance the hydrodynamic resolution even if only three different wavelength signals are evaluated.[12] However, large scale processing of hundreds of distinct wavelengths, which are generated by the MWL detector that records up to 800 separate wavelengths, has been not possible so far. Thus, the outstanding capabilities of the MWL-AUC have not been addressed and could not be exploited until now. Only Ultrascan3 contains the first functionalities to process and fit whole sets of MWL data using for example the 2-dimensional spectrum analysis model, which allows in principle for the extraction of extinction spectra.[13] Even though this model offers many advantages, such as high resolution, accuracy, and the possibility of systematic noise fitting, it also has some drawbacks. For the data evaluation, supercomputing capabilities are required because the direct modeling of the sedimentation process is computationally intensive. Moreover, hydrodynamic or thermodynamic nonideality can result in artifacts in case of an improper direct boundary model, which is not only true for the 2-dimensional spectrum analysis but also for other techniques such as the c(s)-model.[9] Hence, the generation of false positives can impair the result in cases where no prior knowledge is available. Moreover, the correction for diffusion, which is included in these algorithms, is not required for many systems for which diffusion is negligible during the sedimentation process. Furthermore, Ultrascan3 fits each wavelength individually and does not include any further functionalities to process evaluated MWL data, such as the deconvolution of sedimentation profiles. This is, however, required to exploit the maximum potential of MWL-AUC.

For many NPs the sedimentation in the AUC is only slightly affected by diffusion due to their high density and mass (sizes typically >20 nm). For biological macromolecules, the elimination of the effects of diffusion is not desirable for studies on self- or heteroassociation. Such systems would strongly benefit from software allowing for the fast and accurate analysis of MWL data. Until now, only a few MWL-AUCs are available worldwide, but future generations of AUCs such as the centrifugal fluid analyzer (CFA) may further support MWL detection. This will lead to a considerably increased demand for MWL data evaluation in various emerging fields like biology, medicine, chemistry, and nanotechnology.

Here we present a method capable of evaluating and processing MWL data rapidly with low computational effort applicable in numerous applications. We demonstrate our approach for silica and gold NPs which belong to the most widely used NP systems. In principle, the methodology is also applicable to biological macromolecules as it will be shown by means of simulated data. However, due to the optical fiber based design of our MWL-AUC and the reduced sensitivity in the wavelength range below 280 nm we did not focus on such systems in this work.

THEORY

Fundamentals of Sedimentation. In an AUC experiment, a centrifugal field, which can be up to 250,000 times higher than the gravitational field of the earth, is applied to the sample. By overcoming the diffusion acting on the particles, sedimentation according to the particles' mass, size, density, and shape will be induced. Furthermore, interactions between the analytes can affect the hydrodynamics. During a typical SV experiment, the temporal and spatial propagation of the sedimentation boundary from the meniscus to the cell bottom is measured inline using an optical detector. The shape and progress of the sedimentation boundary is given by the sedimentation and diffusion properties of the particles. Absorbance profiles are recorded via radial scans using a CCD-array detector. Since the time needed for one scan is short (~1 min) compared to the overall sedimentation of particles (1–2 h), a single sedimentation profile in the radial dimension can be considered as a snapshot of the analyte distribution in the cell. The movement of the sedimentation boundary contains therefore all information to determine the sedimentation properties of the analytes. The sedimentation coefficient s is defined as the sedimentation velocity u divided by the centrifugal field:

$$s = \frac{u}{\omega^2 r} \tag{1}$$

The strength of the centrifugal field is given by the angular velocity ω and the distance from the axis of rotation r. The sedimentation coefficient s is a unique measure of the hydrodynamic properties of a particle in a given solvent and can be linked to the particle diameter d using Stokes' law:

$$d = \sqrt{\frac{18\eta s}{\rho_p - \rho_s}} \tag{2}$$

The particle size is therefore a function of the sedimentation coefficient, solvent viscosity η, particle density ρ_p, and solvent density ρ_s. By means of eq 2, the particle size distribution can be obtained from the sedimentation coefficient distribution that is the outcome of a SV experiment.

Optical Detection. For an absorbance based measurement, which is also done by the MWL detector in the AUC, the measured quantity is the attenuation of light given by the intensities of the incident light I_0 and the transmitted light I. It can be expressed by Beer–Lambert's law:

$$\log_{10}\frac{I}{I_0} = -\varepsilon c l = -\tau c \tag{3}$$

For a given optical path length l, the extinction depends on the molar or mass concentration c as well as on the extinction coefficient ε of the analyte/particle. Alternatively, the extinction coefficient can be divided by the optical path length, which provides the turbidity τ. The attenuation of light is determined by

DOI: 10.1021/ac504649c
Anal. Chem. 2015, 87, 3396–3403

Scheme 1. Concept of MWL Analysis Using MWL-AUC and SEDANAL[a]

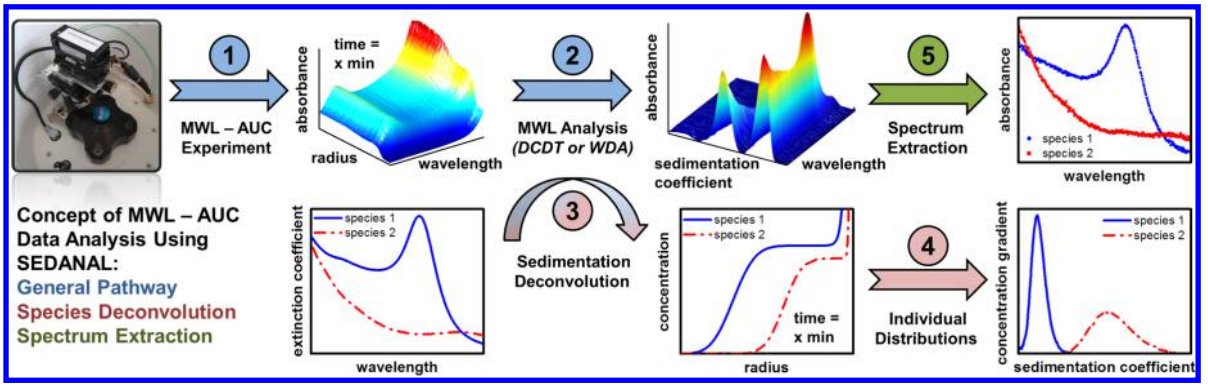

[a]The general pathway (blue) includes the design of the MWL-AUC experiment as well as the measurement and data acquisition in the MWL-AUC. After that two different pathways can be pursued depending on the sample and the existence of prior knowledge. For a mixture of a defined number of species with known optical properties, a deconvolution of the sedimentation data can be done to obtain the sedimentation coefficient distributions of the individual components (red path). Alternatively, the absorbance spectra can be obtained for any sedimentation coefficient and species in case of an arbitrary mixture of species (green path).

the absorbance and scattering of light. It depends on the complex refractive indices of the solvent and the particles under investigation as well as on the density, shape, and size of the particles, which determine whether the extinction is dominated by absorbance or scattering (or both). Hence, the obtained sedimentation coefficient distribution for a MWL-AUC experiment is always extinction weighted but can be converted to a mass weighted distribution as long as the extinction coefficient is known.

The measured extinction in a MWL-AUC experiment will vary with each investigated wavelength according to the different optical properties (extinction spectra that contain an absorbance and a scattering contribution) of the sedimenting analyte. For a given sample and cell, the total analyte concentration and path length will be constant during the experiment. AUC separates the species in the gravitation field, and so any variation of absorbance with wavelength is due to the component sedimenting at that distinct sedimentation coefficient. This is why the optical properties of individual fractions are accessible via MWL-AUC and what we will demonstrate in the following sections.

Analysis of Hydrodynamic Properties. In principle, two different groups of data evaluation routines exist. The first group is based on direct boundary models to assess the change in concentration during the centrifugation. For this, the Lamm equation, which describes the temporal and spatial distribution of the sample due to sedimentation and diffusion, is used by employing least-squares methods according to the popular Todd–Haschemeyer method.[14] By means of different numerical approaches, the distribution of sedimentation, and optionally diffusion, is derived from the raw data. The second group uses model free approaches, such as the van-Holde-Weischet or DCDT analysis.[15,16] The DCDT analysis as implemented in SEDANAL[11] is based on the time derivative approach developed by Stafford to completely remove all the time independent systematic noise such as scratches or dirt on the windows from the data before analysis.[15,17−19] In this work, we will use this model-free approach to integrate the functionalities of MWL data analysis into SEDANAL. The advantage of the DCDT method in comparison to the first group is that due to the direct removal of errors it is direct and model independent. That means it requires no computationally intensive calculations that would otherwise be necessary to fit for the systematic errors. Therefore, large data sets arising from MWL data sets can be easily and rapidly investigated without the need for supercomputing capabilities.

Since the DCDT method has already been described in detail, just a brief overview will be given. The method effectively produces a concentration gradient pattern, dc/ds^* (also called $g(s^*)$), as a function of radius expressed in units of the apparent sedimentation coefficient (not diffusion corrected), s^*. The transformation of the time derivative of the concentration to $g(s^*)$ is given by the following equation[15,17,18]

$$\hat{g}(s^*) \equiv \left(\frac{\partial c}{\partial s^*}\right)_t = \left[\left(\frac{\partial c}{\partial t}\right)_r + 2\omega^2 \int_{s^*=0}^{s^*=s^*} \left(\frac{\partial c}{\partial s^*}\right)_t s^* \mathrm{d}s^*\right]\left(\frac{\partial t}{\partial s^*}\right)_r \tag{4}$$

where s^* is defined by:

$$s^* = \frac{1}{\omega^2 t} \ln\left(\frac{r}{r_m}\right) \tag{5}$$

r_m is the meniscus position, and the other symbols have their usual meaning, as already introduced by the previous equations. The time derivative (DCDT) method uses a subset of scans to give essentially a snapshot of the sedimenting boundary at a particular time during the run and is plotted on a linear s^* scale.[15] In contrast, the wide distribution analysis (WDA) method includes all the scans from a run to give a sedimentation pattern spanning the entire range of s values observable for that run; it is plotted on a log scale to accommodate the wide range of s values observable. In addition, WDA has a multispeed capability allowing extremely wide ranges of the s value to be observed in a single run.[19] In both methods the use of the time derivative eliminates the need to fit for the time independent systematic errors resulting in the elimination of several thousand fitting parameters required by other methods.

Multiwavelength Analysis. Common AUC analysis is based on single wavelength (SWL) absorbance data. Alternatively, interference or fluorescence optics can be applied to determine the sedimentation coefficient distribution. The latter is mainly used for special applications incorporating fluorescent tagged macromolecules and NPs. The conversion of the measured extinction weighted distribution to a mass weighted distribution requires further information regarding the optical properties of the sample. As mentioned in the section about

DOI: 10.1021/ac504649c
Anal. Chem. 2015, 87, 3396−3403

optical detection, the extinction coefficient of the sample is needed to correct for absorbance data. For interference data the refractive index increment dn/dc of the material is needed. However, for complex mixtures of, e.g. different materials, the correlation of sedimentation and optical properties becomes very complex because multiple species may also have multiple extinction coefficients or refractive indices. Thus, the conversion of the measurement data to a quantitative sedimentation coefficient distribution and the distinction of the individual species that contribute to this sedimentation coefficient distribution are hindered.

In contrast to SWL, interference or fluorescence detection, MWL-AUC offers significantly increased information due to the acquisition of numerous wavelengths.[5,20,21] This will change the way AUC data is analyzed and will therefore open completely new possibilities of particle analysis. An overview demonstrating how we treat MWL data in SEDANAL is given in Scheme 1. In the following, the three major advantages of MWL-AUC will be presented:

Increased Signal-to-Noise Ratio. For a single component of known optical properties or multiple components with identical extinction coefficients, the SWL detector can be used to determine all necessary information. Even though in this case the MWL analysis will not provide an increase in information, it will offer statistical advantages. The signal-to-noise ratio (SNR) scales with the square root of number of averages. This means that a MWL analysis using 100 wavelengths can provide a ten times higher SNR in case that the SNR of each scan is in the same order. For experiments at low concentration and data analysis followed up by fitting routines, this offers clear advantages. In this context it has to be noted that wavelengths with a poor SNR used for calculating the average can impair the result. Thus, a major advantage of MWL analysis is that only wavelengths with a similar SNR can be used to gain a significant statistical advantage.

Species Deconvolution. For systems of known optical properties deconvolution of the global sedimentation coefficient distributions can be done to obtain the relative contributions of the individual components/species in the sedimentation coefficient distribution. This represents a highly overdetermined system that can be solved by linear least-squares (LLS) methods. If one has only two components whose spectral properties are well-known and if measurements are available for two wavelengths without any noise, the concentrations of the two components can be simply obtained by algebraically solving two equations for the two unknown component concentrations. However, in the noisy, real world that solution can be quite unstable and very sensitive to the noise. In this context MWL-analysis is seen to be highly promising due to the fact that the overdetermined system is composed of measurements at several hundred wavelengths. This system can be represented by the following linear system which allows us to "blend" all that information into one unique robust solution

$$y = Ac \tag{6}$$

where y is the column vector of absorbance measurements at each of m wavelengths, and A is an m by n matrix of extinction coefficients for the n components at the m wavelengths. c is an n element column vector of component concentrations. n is usually a small integer: 2, 3, 4, etc. The LLS "approximate" solution to this system is easily and quickly obtained by solving this system for c_{LS}, the best linear unbiased estimate of the concentrations of each component at each radius and time point (if the absorbances had no noise, this would be the exact analytical solution). c_{LS} represents the closest solution to the true (i.e., noise-free) values of the concentration in the least-squares sense:

$$c_{LS} = (A^T A)^{-1} A^T y \tag{7}$$

This system, comprising as many as m = 500 wavelengths, is solved repeatedly at each time point and at each radial position to deconvolute the n concentration vs radius curves using the FORTRAN LAPACK and BLAS routine, DGELSY, in SEDANAL, for solving linear systems. The Linear Algebra Package (LAPACK 3.5.0) and Level 3 BLAS subroutines are open source code and can be obtained from http://www.netlib.org/lapack/ and http://www.netlib.org/blas/, respectively.

Spectrum Extraction. According to the Beer−Lambert's law, the optical density (OD) at a fixed optical path length is a product of the extinction coefficient and the concentration. Consequently, the peak area of the sedimentation coefficient distribution which contains information on all analytes in the measurement cell is proportional to the extinction coefficient and loading concentration of the material. For multiple components that show well distinguishable sedimentation coefficient peaks, the peak areas are separated from each other and can be considered individually. Thus, the MWL evaluation provides the wavelength-dependent peak areas. Since the concentration is constant and independent of the wavelength under consideration, any differences in the peak areas are proportional to the extinction coefficients of the individual species. Accordingly, by means of MWL analysis, the optical properties (extinction spectra) of the individual species can be derived without the need of time-consuming purification. For consideration of individual species, this requires that the peaks in the sedimentation coefficient distributions of the species are clearly recognizable. However, for a continuous distribution the spectra can also be extracted as a function of the sedimentation coefficient and particle size to investigate spectral size dependencies even though the signal could be superimposed by two different materials depending on the sample composition. For chemically identical particles of different size this will directly provide the size dependent spectral properties.

EXPERIMENTAL SECTION

AUC Measurements. A modified preparative centrifuge, type Optima L-90K, available from Beckman Coulter has been used for the sedimentation velocity experiments. Further information regarding the applied MWL optics as well as the data acquisition can be found in the literature.[5,7] Titanium centerpieces (Nanolytics, Germany), path length 12 mm, were used for all experiments. The temperature was set to 20 °C for all measurements and was held constant for at least 1 h before starting the experiment. Sedimentation velocity data has been acquired at 4 krpm for the silica-gold mixture and 3 krpm for the gold mixture, which provided well-resolved SV data.

Absorbance Measurements. Extinction coefficients were determined via absorbance measurements using a Cary 100 Scan UV/vis spectrophotometer (Varian GmbH, Germany) with spectral steps of 1 nm. The mass concentration of the silica NPs was taken from the data of the manufacturer. The mass concentration of the gold NPs was calculated assuming a conversion of 100% during the synthesis.

Simulated Sedimentation of Proteins. Sedimentation profiles were simulated for bovine serum albumin (BSA) and β-lactoglobuline (BLG) for several wavelengths with the extinction coefficients measured separately for both proteins. Sedimenta-

DOI: 10.1021/ac504649c
Anal. Chem. 2015, 87, 3396−3403

tion profiles of the BSA/BLG mixture were simulated for 50 krpm with a time interval of 100 sec. Simulation parameters were as follows: M = 18.4 kg/mol, s = 2.0 sved, $d\rho/dc$ = 0.268 for BLG and M = 66.1 kg/mol, s = 4.3 sved, $d\rho/dc$ = 0.268 for BSA. Gaussian random noise with a standard deviation of 1% was added to the data.

Silica Nanoparticles. Blue colored silica "sicastar-blue" NPs (Micromod Partikeltechnology GmbH, Germany) with a size of 100 nm (#73-00-102) were used as purchased, and concentrations were adjusted via dilution using ultrapure water (18.2 MΩ cm^{-1}; total oxidizable carbon <10 ppb). Silica particles incorporating a blue dye were chosen over white silica particles as an illustration because of the spectral features, which can be detected by MWL-AUC.

Syntheses of Gold Nanoparticles. For the mixture with silica particles, small gold NPs were synthesized according to the method of Turkevich et al.[22−25] 7.3 mL of an aqueous solution of 5.5 mM $NaAuCl_4$ was added to 100 mL of boiling H_2O. After further boiling, 12.5 mL of an aqueous solution of 19.4 mM trisodium citrate was added leading to the formation of gold NPs about 15 nm in size. Larger sized gold NPs were produced via seed-growth synthesis. The Au seeds were synthesized by adding 1 mL of 25 mM $NaAuCl_4$ into 150 mL of boiling 2.2 mM trisodium citrate. After the synthesis of the Au seeds in 10 min, the reaction solution was cooled down to 90 ± 1 °C. Then, 1 mL of 60 mM trisodium citrate and 1 mL of 25 mM $NaAuCl_4$ were consecutively added to the solution with a time delay of ∼2 min. After 30 min, the reaction was completed, and a sample of 2 mL was extracted. This process was repeated in order to get different sizes of Au NPs. For the preparation of the 2-component mixture of gold particles we used the seed particles and one larger size fraction, which were prepared according to the methodology described before. Scanning electron microscopy (SEM) and image analysis were applied prior to the AUC experiment to verify that species of different size were obtained. For the larger NPs we estimated the mean mass weighted particle size. The seed particles were too small for a SEM analysis.

Data Analysis. MWL data analysis was carried out using SEDANAL. The SEDANAL preprocessor can read the MWL files created by the MWL-AUC machine (binary format with one file per scan containing all the wavelengths) to create a single "run" file. This run file contains all scans from all wavelengths in addition to meta-data like the meniscus and the base radii that were chosen in the preprocessor. In the next step, either DCDT or WDA is chosen to display the sedimentation pattern either as $g(s^*)$ vs s^* for narrow distributions[15] or as $s^*g(s^*)$ vs $\ln(s^*)$ for both narrow and very wide single or multispeed distributions,[19] respectively. In what follows, please note the following equivalences: $g(s^*) = da/ds^*$ and $s^*g(s^*) = da/d\ln(s^*)$. In the following, we use absorbances a instead of concentrations since this is the customary parameter of the MWL-AUC. For either DCDT or WDA analysis the user can choose distinct or all wavelengths for the distribution plots.

In principle, absorption spectra can be obtained for a fixed sedimentation coefficient by plotting the different absorbances derived from the DCDT or WDA analysis as a function of the wavelength. However, since the time derivative patterns contain noise, a smoothed spectrum is obtained from the patterns by integrating over a range of sedimentation coefficient values to get an absorbance or extinction, a, over that range. The same range is used for each wavelength. For DCDT we have

$$a(\lambda) = \int_{s_1^*}^{s_2^*} \left(\frac{\partial a}{\partial s^*}\right)_\lambda ds^* \tag{8}$$

and, similarly, for WDA we have:

$$a(\lambda) = \int_{s_1^*}^{s_2^*} \left(\frac{\partial a}{\partial \ln(s^*)}\right)_\lambda d\ln(s^*) \tag{9}$$

These absorbances can then be plotted as a function of the wavelength to produce the spectrum. Any particular spectrum must finally be normalized by the appropriate molar or mass concentration to get the extinction coefficients. Vice versa, molar or mass concentrations can be calculated for known extinction coefficients. The values of s_1^* and s_2^* are chosen to include as much of each peak as possible without having significant overlap with any neighboring peaks.

Deconvolution of Component Concentration Profiles from MWL Data Sets. After solving the linear system from the large MWL data set, the column vector c_{LS} will contain the concentrations of each of the n components in the mixture. SEDANAL will then write out the concentration profiles to n series of scan files in XL-A/I format of the commercial AUC by Beckman-Coulter. It is written one file for each time point and/or stored as n "run" files readable by SEDANAL. Thus, they can be processed by DCDT and WDA to produce the corresponding sedimentation patterns for the individual components and by the SEDANAL fitter which is used to fit to various appropriate models. The deconvoluted concentration vs radius files in XL-A/I format can also be read by other software programs employing other types of analysis methods.

RESULTS AND DISCUSSION

Simulated Data. At first, a set of simulated data was considered to test the functionality of the MWL SEDANAL analysis with synthetic data. The resulting sedimentation profiles are given in Figure 1c. As known from literature, BSA sediments faster due to its higher molar mass, whereby broadening of the boundary is slightly more enhanced for BLG due to its lower hydrodynamic diameter and higher diffusion coefficient. Even though the extinction coefficients are similar but not identical for the proteins as shown in Figure 1a, the sedimentation profiles could be readily deconvoluted. The plateau concentrations at 10,000 sec are about 15−20% lower than the loading concentrations of 1.0 g/L. This is ascribed to radial dilution in the sector shaped cell. In the next step, both patterns can be evaluated individually with any desired software as usual to provide the sedimentation coefficient distributions of BSA and BLG.

Our methodology is independent of the considered spectral range. Even though deep UV-data cannot be generated with the current MWL detector, future generations of MWL-AUC will provide this opportunity. This in turn will require appropriate data analysis tools, such as presented in this work, to take advantage of the manifold possibilities in biological and medical applications.

Mixture of Silica and Gold Nanoparticles. After showing the functionality of our methodology for simulated data, the possibilities of MWL analysis will be demonstrated by means of a mixture of blue colored silica and reddish colored gold NPs, about 100 and 15 nm in size, respectively. The extinction spectra of the two NPs were measured, and extinction coefficients were then calculated based on the known concentrations for both particles before mixing. The obtained data is provided in Figure

DOI: 10.1021/ac504649c
Anal. Chem. 2015, 87, 3396−3403

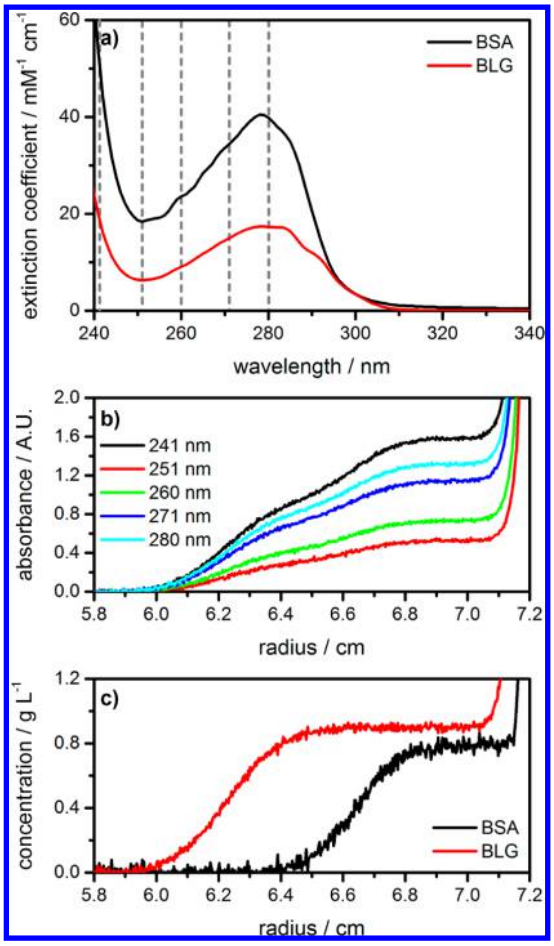

Figure 1. a) Extinction coefficients of BSA and BLG used for the generation of simulated sedimentation profiles. Selected wavelengths for deconvolution of sedimentation data are indicated by vertical dashed lines. b) Synthetic sedimentation profiles of the BSA-BLG mixture after 10,000 sec and 50 krpm for 5 different wavelengths. c) Deconvoluted sedimentation profiles for BSA and BLG based on the simulated wavelengths shown in b).

2a. It can be seen that the profiles are quite different for the two species. The smaller gold NPs have high extinction coefficients in the visible range of the spectrum and show a unique spectral feature at 520 nm. Noteworthy, this causes the reddish color of the dispersion. The peak position can be correlated to the diameter of the particle due to the well-known surface-plasmon resonance of the noble metal. In contrast, the extinction coefficients of the blue colored silica NPs are much smaller and show no significant features in the UV/vis spectrum. Only a weak peak at 600 nm can be assigned to the blue color of the NPs. Besides, the extinction is dominated by scattering and increases to the UV in accordance to Rayleigh scattering.

A sedimentation velocity experiment was performed at 4 krpm for a mixture of both NPs. Already the raw data of the MWL experiment, of which a snapshot is given in Figure 2b, reveals the two species with their different sedimentation coefficients and optical properties. As it can be seen, the sedimentation velocity of the silica NPs is much higher compared to the gold NPs. A movie of the sedimentation experiment can be found in the Supporting Information (SI).

The sedimentation data was evaluated using the DCDT method, which resulted in 329 distributions, one for each wavelength. In Figure 2c as an example, the extinction weighted distribution evaluated at 520 nm is given. The peak positions of the two species are well separated. According to the raw data, the first peak has to correspond to the slower sedimenting gold NPs. We deconvoluted the sedimentation data using the extinction coefficients and MWL data to obtain the individual distributions of the two species. The distribution of the silica NPs shows a "wiggle" at the peak position of the distribution of gold. So far, we cannot fully explain the reason for this feature. The origin of this effect is under investigation and will be reported at a later time. However, it has to be noted that this artifact seems to have no noticeable influence on the final distribution because the shape of the gold NPs distributions is preserved after deconvolution of the data. Moreover, the average peak area of this wiggle is zero. Thus, it is canceled during the integration, and the spectra can still be extracted despite this effect.

Furthermore, and according to step 5 in Scheme 1, the peak areas of the convoluted distribution were calculated via integration and plotted vs the wavelength to retrieve the extinction spectra of the two species from the AUC measurement. The final, normalized spectra of the species and their retrieved spectra are shown in Figure 2d. For both particles the spectra match very well. For the retrieved spectrum of the silica NPs an increase in absorption is found around 520 nm, which is in the range of the peak maximum of the gold spectrum. Since both sedimentation coefficient peaks were sufficiently separated, we believe that this may be attributed to a small amount of gold NPs bound to some of the silica NPs.

In summary, we are able to show for the first time that it is possible to determine the individual extinction spectra of two species in a multicomponent mixture using MWL-AUC and one single sedimentation velocity experiment, which took no longer than 1 h. For this, no purification of the sample was required. It also needs to be pointed out that the entire analysis was completed within a few minutes on a standard notebook or office computer.

Mixture of Gold Nanoparticles. To further emphasize the sensitivity of MWL-AUC to hydrodynamic and spectral properties, we investigated a second mixture containing two differently sized gold NPs. The size of the NPs is expected to be in the range of 10 to 30 nm according to the peak maxima of the spectra. A red-shift of the peak maxima with increasing particle size will be caused by the surface-plasmon resonance.

Herein, we did not aim to deconvolute the sedimentation coefficient distributions based on the extinction coefficients of the individual fractions but wanted to extract instead the individual extinction spectra. For many applications, optical properties of particles are needed but not known because the signals of individual fractions are superimposed by the signal of other components in the mixture. Thus, tedious purification protocols have to be carried out to obtain the individual species and to measure their absorbance spectra. With MWL-AUC most of these protocols will become unnecessary because optical information can be extracted for different sedimentation coefficients and species directly.

In Figure 3a the obtained sedimentation coefficient distribution as a function of the wavelength is shown. We observed two major species with average sedimentation coefficients of 1476 and 5706 sved, which translates to particle sizes of 12.1 and 23.7 nm, respectively. The value of the larger species agrees well with the results by SEM analysis, which provided a mean value of about 21 nm. Herein, it has to be mentioned that the AUC analysis will provide much more accurate results than the SEM due to its superior resolution and statistics. For both species we

DOI: 10.1021/ac504649c
Anal. Chem. 2015, 87, 3396−3403

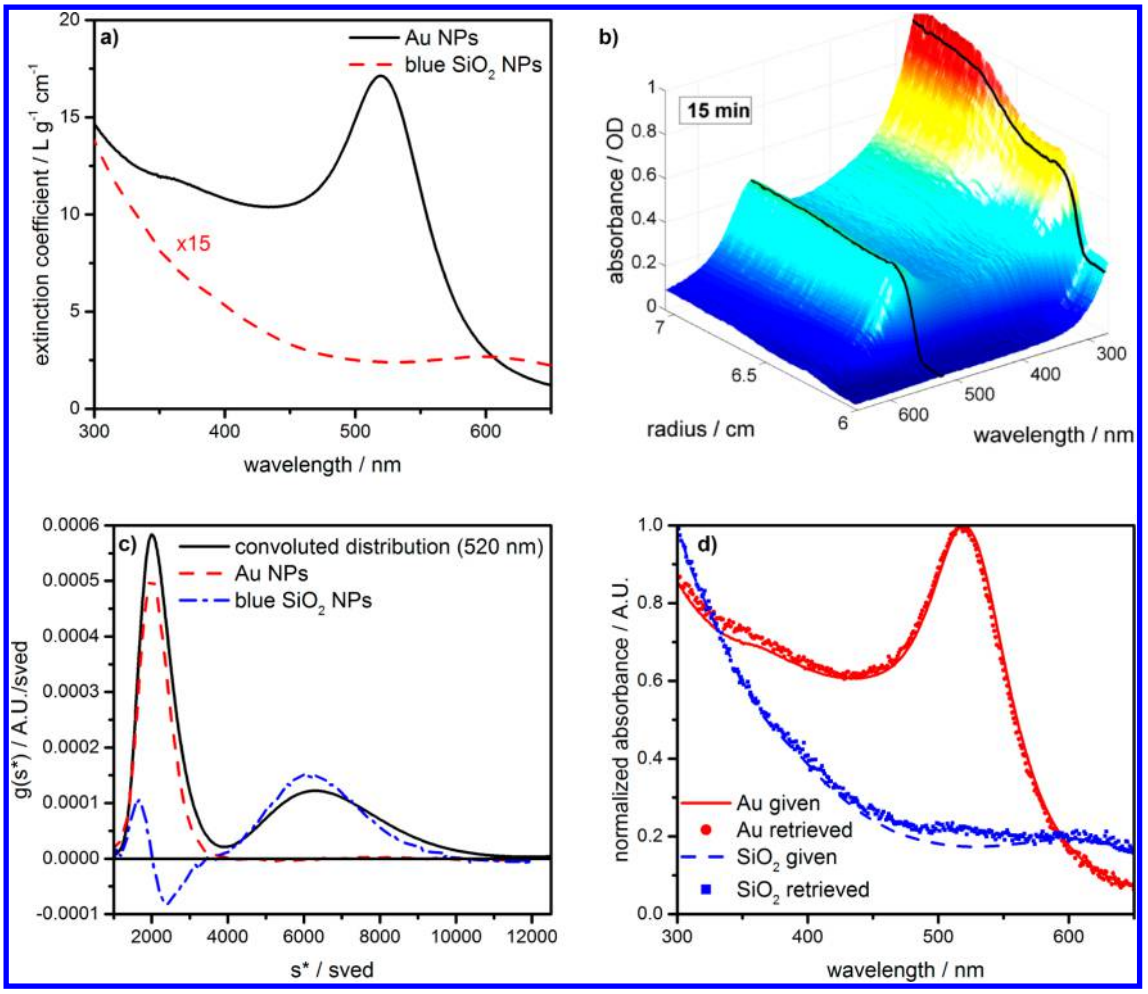

Figure 2. a) Extinction coefficients of the silica and gold NPs. The extinction coefficient of the silica NPs was multiplied by 15 to be better recognizable. b) Multiwavelength spectra of the silica-gold mixture sedimenting at 4 krpm in a sedimentation velocity experiment as a function of the radial distance from the axis of rotation. The scan was taken after 15 min. Two different wavelengths corresponding to the spectral features of the two species were highlighted with black lines as a guide to the eye. c) Convoluted sedimentation coefficient distributions at 520 nm and deconvoluted sedimentation coefficient distributions of gold and silica NPs. 329 wavelengths values were used for the MWL analysis. The distributions were not normalized for the sake of clarity. d) Extinction spectra of the two species measured using a benchtop UV/vis spectrometer as well as the extinction data reproduced from the MWL AUC experiment. Spectra were normalized to a maximum value of one to be comparable.

further extracted the extinction spectra (Figure 3b). As expected from Mie's theory, the peak position shifts about 3 nm for the larger gold NPs.[26] A movie showing the size dependent spectra of the gold NPs can be found in the SI. Due to the high sensitivity of the AUC toward the sedimentation behavior of NPs and thus the particle size as well as the high spectral resolution, we believe that MWL-AUC will become a powerful tool for the simultaneous analysis of hydrodynamic and optical properties.

■ CONCLUSIONS

Our developments enable us to do a fast and accurate analysis of multiwavelength (MWL) data obtained by the analytical ultracentrifuge (AUC). The possibility of MWL analysis will be of high benefit for biomedical applications and nanotechnology. MWL-AUC offers a much higher statistical confidence compared to single wavelength analysis due to the evaluation at multiple wavelengths. Furthermore, the individual extinction spectra of species in complex mixtures become accessible by means of a MWL evaluation. This will have considerable impact for applications in photonics and nanotechnology, where structure−property relations such as the size dependent optical properties of particles are investigated. Without MWL-AUC very time-consuming purification protocols have to be applied − provided they exist at all − to isolate individual fractions from mixtures to study their optical properties. MWL-AUC offers such information in only one experiment making it a highly effective technique. Deconvolution of the concentration profiles allows for the determination of the individual sedimentation coefficient distributions of species in a mixture. The deconvolution method requires all the extinction coefficients and depends on the components having "sufficiently" different spectra. What "sufficient" for distinct samples actually means will depend to a large extent on the signal-to-noise ratio of the data.

Further studies shall be focused on the development of MWL-analysis for direct boundary models, which would allow for the fitting of radius-independent noise and meniscus positions. Moreover, it would be desirable to develop MWL analysis which is able to deconvolute diffusion. Very small nanoparticles such as semiconductor quantum dots would clearly benefit from such developments because assignment of the hydrodynamic and optical properties is hindered by diffusional broadening. However, for all systems where diffusion plays a negligible role

DOI: 10.1021/ac504649c
Anal. Chem. 2015, 87, 3396−3403

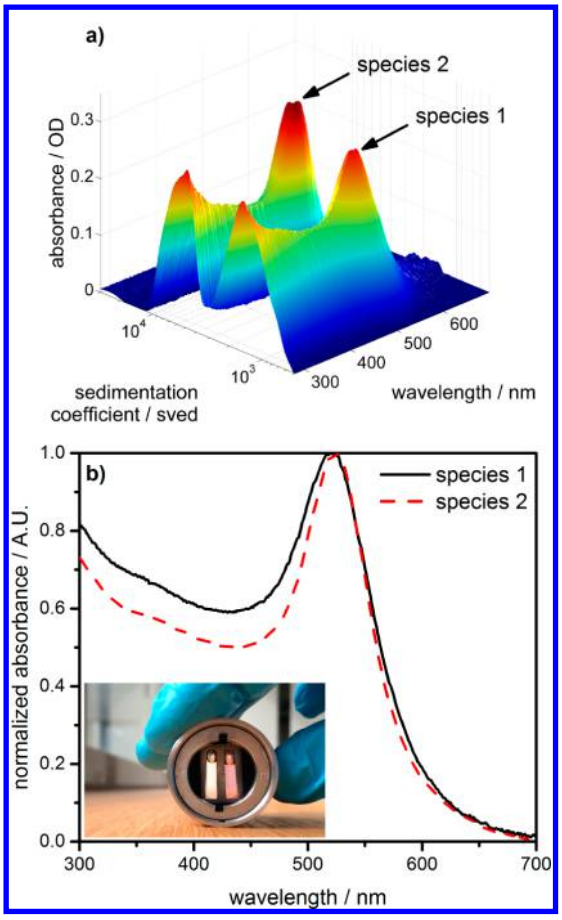

Figure 3. a) 3D-plot of sedimentation coefficient distribution of the gold NPs mixture vs their extinction spectra. b) Normalized extracted extinction spectra for the two differently sized gold NP fractions. A slight peak shift of about 3 nm is observed for the larger species.

(large particle sizes) and therefore does not need to be taken into account, we have presented a fast and reliable methodology. We believe that this will be of large benefit for numerous applications in nano- and biotechnology.

Multiwavelength capabilities are currently integrated into the next version of SEDANAL, which can be obtained for free via http://www.sedanal.org/.

■ ASSOCIATED CONTENT

Ⓢ Supporting Information

Movie of the sedimentation velocity experiment of the silica-gold nanoparticle mixture and movie of the size dependent spectra of the gold nanoparticle mixture. This material is available free of charge via the Internet at http://pubs.acs.org.

■ AUTHOR INFORMATION

Corresponding Authors

*E-mail: wolfgang.peukert@fau.de (W.P.).
*E-mail: wstafford3@walterstafford.com (W.F.S.).

Notes

The authors declare no competing financial interest.

■ ACKNOWLEDGMENTS

The authors would like to thank Deutsche Forschungsgemeinschaft (DFG) for their financial support within the framework of its "Excellence Initiative" of the Cluster of Excellence "Engineering of Advanced Materials" at Friedrich-Alexander-Universität Erlangen-Nürnberg (FAU). The DFG is also thanked for financial support through project "PE 427/28-1". Christoph Metzger and Ulrike Weichsel are thanked for help during the development of the protocol for gold NP synthesis.

■ REFERENCES

(1) Scott, D. J.; Harding, S. E.; Rowe, A. J. *Analytical Ultracentrifugation: Techniques and Methods*; Royal Society of Chemistry; 2005.
(2) Mächtle, W.; Börger, L. *Analytical Ultracentrifugation of Polymers and Nanoparticles*; Springer-Verlag: Berlin, Heidelberg, 2006.
(3) Cole, J. L.; Lary, J. W.; Moody, T. P.; Laue, T. M. *Methods Cell Biol.* **2008**, *84*, 143−179.
(4) Mächtle, W. *Biophys. J.* **1999**, *76*, 1080−1091.
(5) Walter, J.; Löhr, K.; Karabudak, E.; Reis, W.; Mikhael, J.; Peukert, W.; Wohlleben, W.; Cölfen, H. *ACS Nano* **2014**, *8*, 8871−8886.
(6) Walter, J.; Nacken, J. T.; Damm, C.; Thajudeen, T.; Eigler, S.; Peukert, W. *Small* **2015**, *11*, 814−825.
(7) Bhattacharyya, S. K.; Maciejewska, P.; Börger, L.; Stadler, M.; Gülsün, A. M.; Cicek, H. B.; Cölfen, H. In *Analytical Ultracentrifugation VIII*; Wandrey, C., Cölfen, H., Eds.; Springer-Verlag: Berlin, Heidelberg, 2006; pp 9−22.
(8) Strauss, H. M.; Karabudak, E.; Bhattacharyya, S.; Kretzschmar, A.; Wohlleben, W.; Cölfen, H. *Colloid Polym. Sci.* **2008**, *286*, 121−128.
(9) Schuck, P. *Biophys. J.* **2000**, *78*, 1606−1619.
(10) Stafford, W. F. In *Current Protocols in Protein Science*; John Wiley & Sons, Inc.: 2003.
(11) Stafford, W. F.; Sherwood, P. J. *Biophys. Chem.* **2004**, *108*, 231−243.
(12) Balbo, A.; Minor, K. H.; Velikovsky, C. A.; Mariuzza, R. A.; Peterson, C. B.; Schuck, P. *Proc. Natl. Acad. Sci. U. S. A.* **2005**, *102*, 81−86.
(13) Brookes, E.; Cao, W.; Demeler, B. *Eur. Biophys. J.* **2010**, *39*, 405−414.
(14) Todd, G. P.; Haschemeyer, R. H. *Proc. Natl. Acad. Sci. U. S. A.* **1981**, *78*, 6739−6743.
(15) Stafford, W. F. *Anal. Biochem.* **1992**, *203*, 295−301.
(16) Van Holde, K. E.; Weischet, W. O. *Biopolymers* **1978**, *17*, 1387−1403.
(17) Stafford, W. F. *Methods Enzymol.* **1994**, *240*, 478−501.
(18) Stafford, W. F. *Methods Enzymol.* **2000**, *323*, 302−325.
(19) Stafford, W. F.; Braswell, E. H. *Biophys. Chem.* **2004**, *108*, 273−279.
(20) Karabudak, E.; Backes, C.; Hauke, F.; Schmidt, C. D.; Cölfen, H.; Hirsch, A.; Wohlleben, W. *ChemPhysChem* **2010**, *11*, 3224−3227.
(21) Karabudak, E.; Wohlleben, W.; Colfen, H. *Eur. Biophys. J.* **2010**, *39*, 397−403.
(22) Turkevich, J.; Stevenson, P. C.; Hillier, J. *Discuss. Faraday Soc.* **1951**, *11*, 55−75.
(23) Kimling, J.; Maier, M.; Okenve, B.; Kotaidis, V.; Ballot, H.; Plech, A. *J. Phys. Chem. B* **2006**, *110*, 15700−15707.
(24) Frens, G. *Kolloid-Z. Z. Polym.* **1972**, *250*, 736−741.
(25) Frens, G. *Nature* **1973**, *241*, 20−22.
(26) Mie, G. *Ann. Phys.* **1908**, *330*, 377−445.

DOI: 10.1021/ac504649c
Anal. Chem. 2015, 87, 3396−3403